CHARACTERISTICS OF X-RAY RADIATION FROM A GAS-PUFF Z-PINCH PLASMA

N. Akiyama[+] and K. Takasugi

Atomic Energy Research Institute, Nihon University
[+]College of Science and Technology, Nihon University
1-8-14 Kanda-surugadai, Chiyoda-ku, Tokyo 101-8308, JAPAN

ABSTRACT

Characteristics of x-ray radiation from Ar gas-puff z-pinch plasma have been investigated by changing delay time of discharge from gas puffing. Intense cloud structure of x-ray image was observed at small delay time region, but the total x-ray signal was not so intense. The x-ray signal increased with increasing the delay time, and hot spots of x-ray image also became intense. Electron temperature was evaluated from x-ray spectroscopic data, and no significant difference in temperature was observed.

I. Introduction

Gas-puff z-pinch is easy in handling, and is used as a repetitive x-ray radiation source. The efficiency of energy transfer to the plasma is high,[1)] and it is expected as a high power radiation source. Several operating regions exist for the gas-puff z-pinch plasma depending on the delay time of discharge from gas puffing.[2)] Cloud structure of x-ray image has been observed near vacuum discharge region.

X-ray spectroscopy near He-like resonance line of Ar ion has been investigated, and K_α line of Fe atom has been observed.[3)] Satellite lines have also been observed in the long wavelength side of the resonance line. Intensity ratio of Li-like satellite line to He-like resonance line is a simple function of electron temperature.[4-6)] Here the electron temperature is evaluated according to the model, and investigated for different delay times.

II. Experimental Setup

The SHOTGUN gas-puff z-pinch device used in the experiment is shown in Fig. 1. The capacitance of the main bank is 24 μ F, which is charged up to 25kV (7.5kJ). The distance between the electrodes is 30mm. Annular gas is injected through a hollow gas nozzle mounted

on the anode. The diameter of gas nozzle is 28mm. Ar gas is used in the experiment. The gas pressure or the density simply increases with time from gas puffing. We define the time of discharge from gas puffing as "delay time". Discharge currents are detected by Rogowski coils located at the entrance of the chamber (anode) and on the cathode. The cathode current represents discharge current between the electrodes.

The devices used for the measurement of x-ray radiation are scintillation probes, an x-ray spectrograph and a pinhole camera. The scintillation probe used here is filtered by 10 μm Be foil and it can take temporal x-ray signal with energy exceeding 1keV. The pinhole camera can take four plasma images simultaneously with different filters, 5 μm Be ($E > 1$ keV), 15 μm Al ($E > 3$ keV), 100 μm Al ($E > 8$ keV), and 500 μm Al ($E > 12$ keV). A Johansson type spectrograph with a curved quartz crystal ($2d = 6.62$ Å) is used for x-ray spectroscopy around He-like resonance line of Ar ions. The radius of Rowland circle is 250 mm. The x-ray film used both for spectroscopy and pinhole photography is Kodak DEF film.

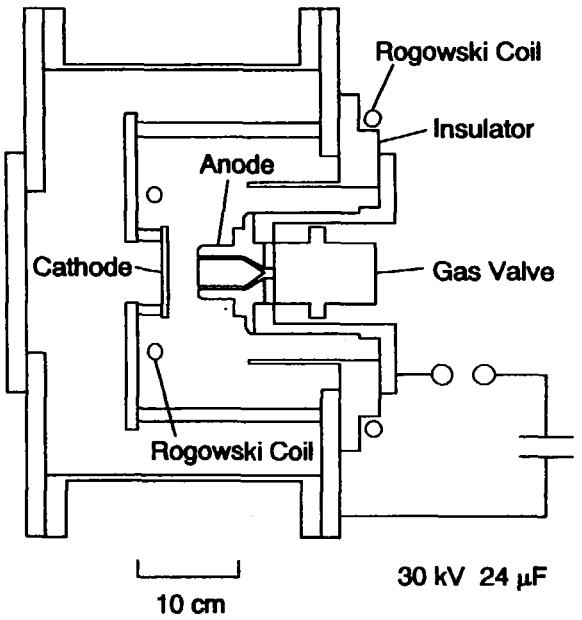

Fig. 1 The SHOTGUN gas-puff z-pinch device.

III. X-ray Spectra

The x-ray radiation of He-like and Li-like ions is analyzed based on Refs. 4 - 6. The excited state of He-like resonance line is excited by collisional excitation and dielectronic recombination. The intensity of He-like resonance line is

$$I = N_{He} N_e (C + D) \ , \tag{1}$$

where N_{He} and N_e are densities of He-like ion and electron respectively. The rate coefficients C and D are collisional excitation and dielectronic recombination.

The excited state of Li-like satellite line is populated by dielectronic recombination of He-like ion. This level is depopulated by autoionization and radiation. The intensity of Li-like satellite line is

$$I_s = N_{He} N_e C_d \frac{A_r}{(A_a + A_r)} \quad , \tag{2}$$

where C_d is dielectronic recombination rate, A_a is autoionization rate, and A_r is radiation rate. The intensity ratio of Li-like satellite line and He-like resonance line is

$$\frac{I_s}{I} = \frac{1.048 \times 10^{-17}}{1+\alpha} \frac{E_0}{T} \frac{1}{fP} \exp\left\{\frac{E_0 - E_s}{T}\right\} \times g_s \frac{A_a A_r}{A_a + \Sigma A_r} \quad , \tag{3}$$

where E_0 and E_s are energies of He-like resonance line and Li-like satellite line respectively, and T is electron temperature. The factor g_s is statistical weight of the excited level, f is oscillator strength, P is Gaunt factor, and $\alpha = D/C$. The summation is taken over related levels.

In the experiment several satellite lines are observed in the same wavelength region. Here we used three lines, j, k, and l defined in Ref. 4. The total intensity ratio of relating lines as a function of temperature is shown Fig. 2. The ratio decreases monotonically with temperature.

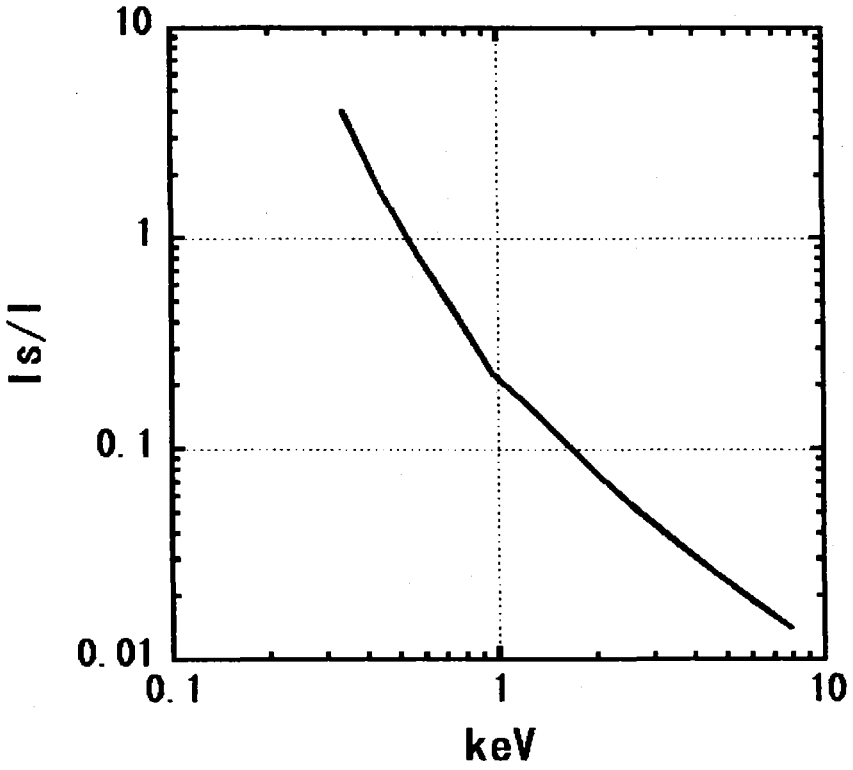

Fig. 2 Line intensity ratio vs. electron temperature.

IV. Experimental Results

Typical current waveforms and x-ray signal detected by a scintillation probe are shown in Fig. 3. As the z-pinch column shrinks, its inductance increases, and the dip is formed in the current waveform. The moment of x-ray pulse corresponds to this current dip. Let's define "pinch time" as the time interval between the start of discharge and the x-ray pulse. As the delay time increases, the pinch time also increases (Fig. 4). This is due to the increment of pinch mass. Net input energy into the pinch column is obtained from the current waveform[3] and is shown in Fig. 5. The energy increases with the delay time.

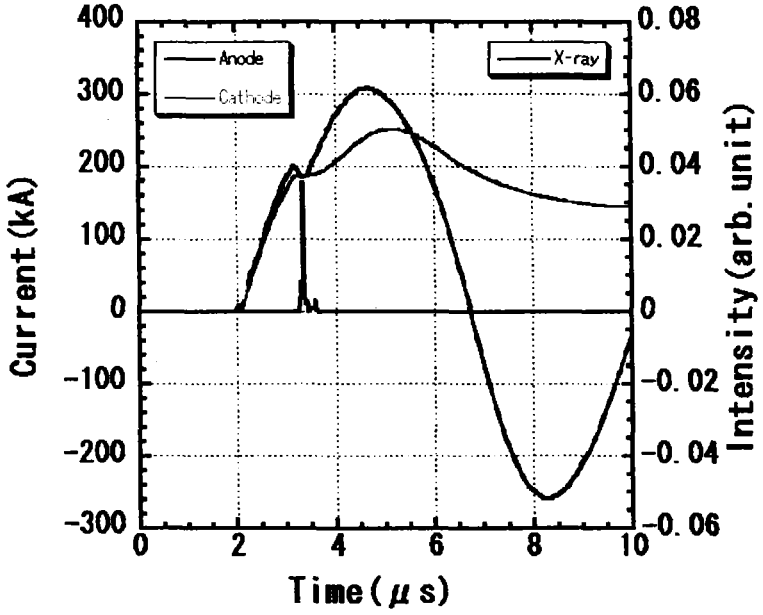

Fig. 3 Typical current waveforms and x-ray signal.

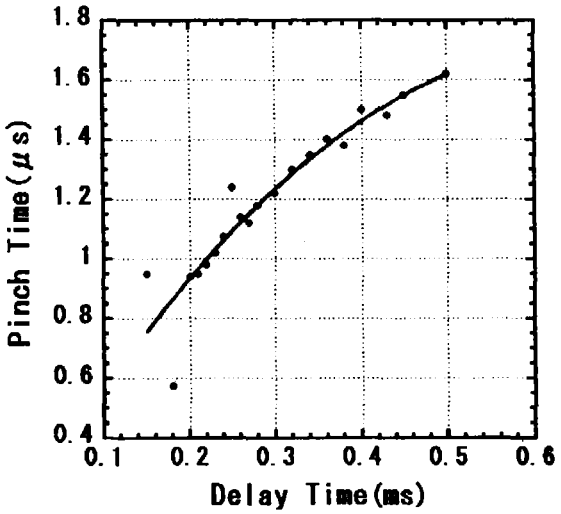

Fig. 4 Pinch time vs. delay time.

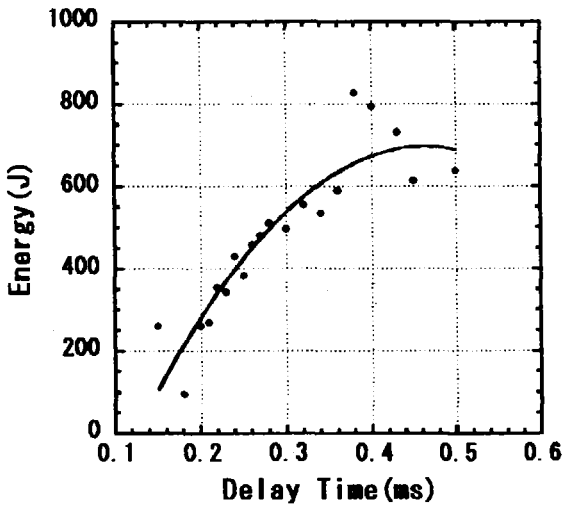

Fig.5 Net input energy vs. delay time.

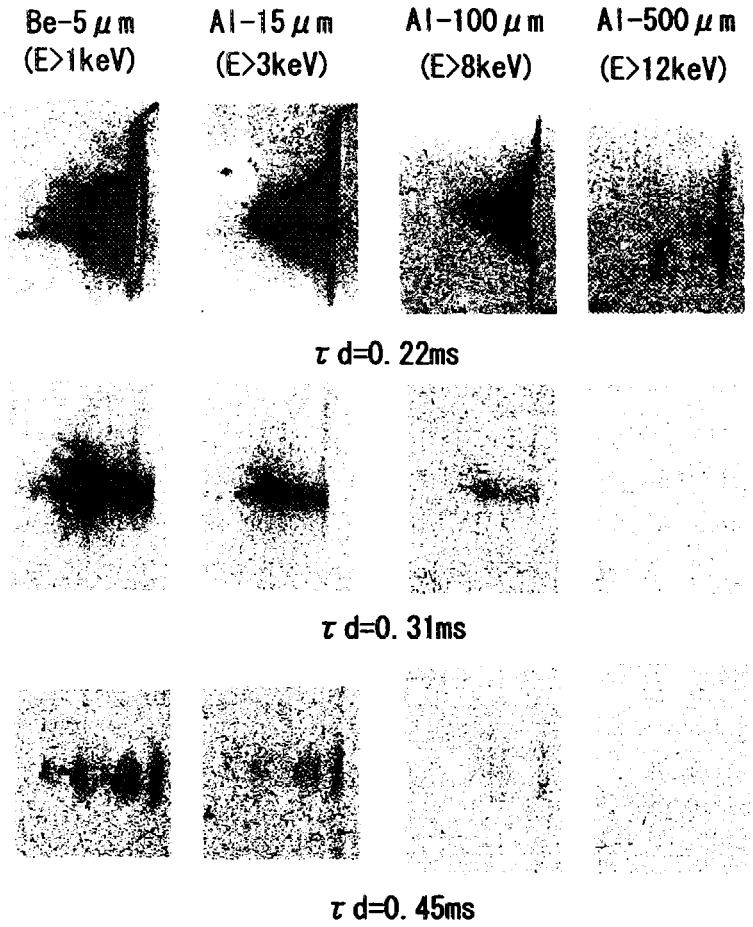

Fig. 6 X-ray pinhole photographs at different delay times.

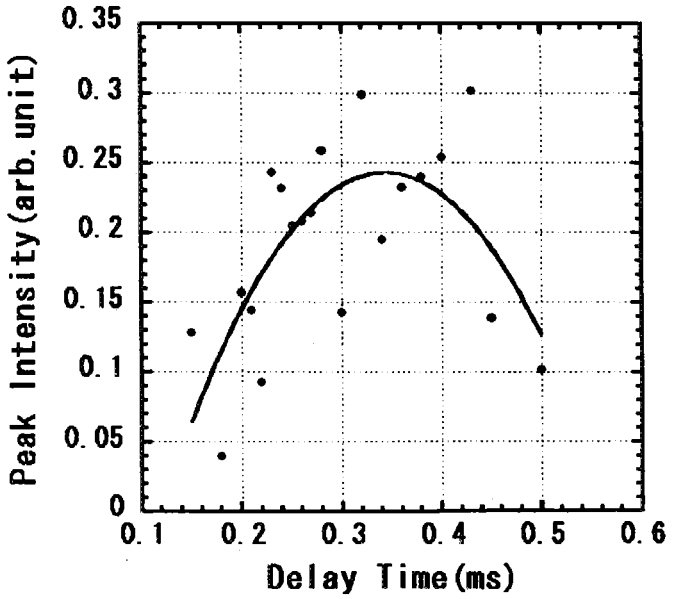

Fig. 7 X-ray intensity vs. delay time.

X-ray images taken by the pinhole camera is shown in Fig. 6 for three different delay time τ_d. Cloud structure of the x-ray is obvious and hard component of x-ray (Al-500 μm) is observed on the surface of anode at short delay time (τ_d = 0.22 ms). With increasing the delay time the hard component of x-ray decreases, and hot spots becomes intense. Figure 7 shows peak intensity of x-ray detected by a scintillation probe. The signal increases with the delay time up to 0.4 ms. Further increasing the delay time, the x-ray intensity drops.

X-ray spectra and its intensity are shown in Fig. 8. The strongest line is Ar XVII He-like resonance line (3.9488 Å). The next lines to long wavelength side are Ar XVII He-like intercombination line (3.9691 Å), Ar XVI Li-like satellite line (3.989 Å), and Ar XV Be-like satellite line (4.010 Å). The lines observed to the left are not from Ar but from Fe. The lines around Fe K_α line (1.938 Å) are observed by secondary reflection of the crystal.[3)]

The electron temperature is evaluated using the intensity ratio of Eq. (3). In Fig. 9 the temperature is plotted against the delay time. The temperature is distributed around 1 keV, and there is no systematic tendency with the delay time.

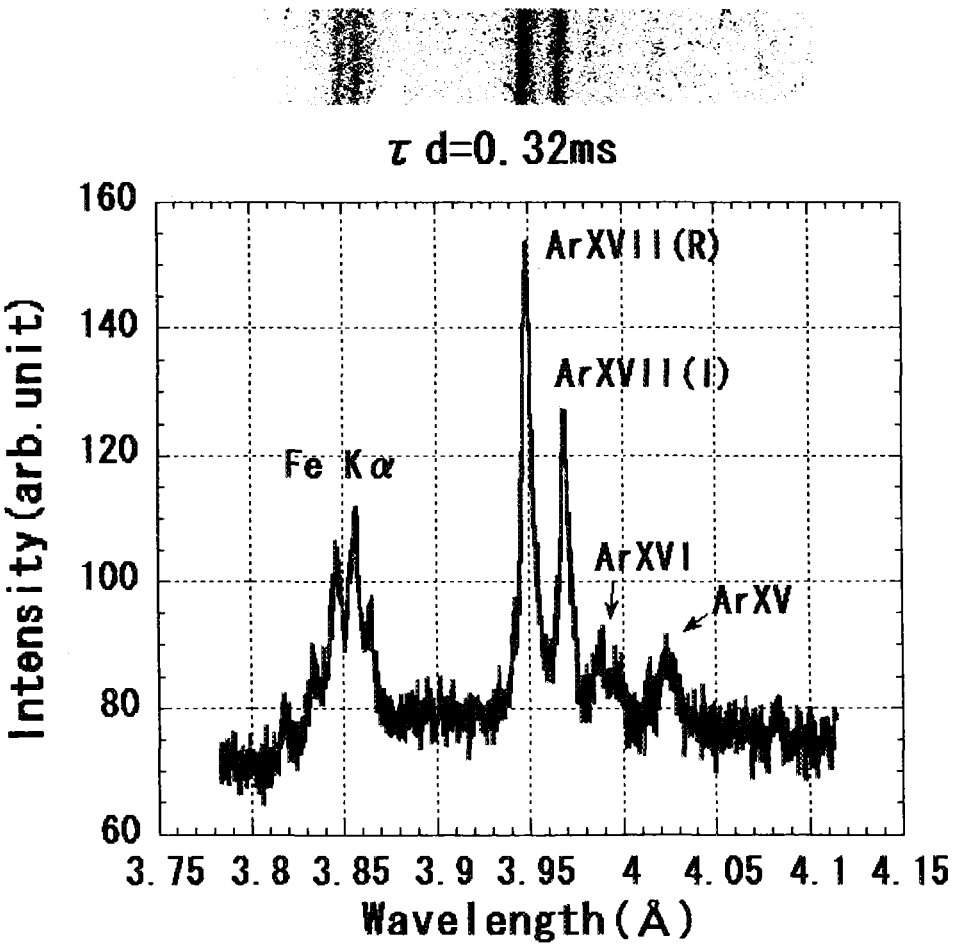

Fig. 8 X-ray spectra and its intensity.

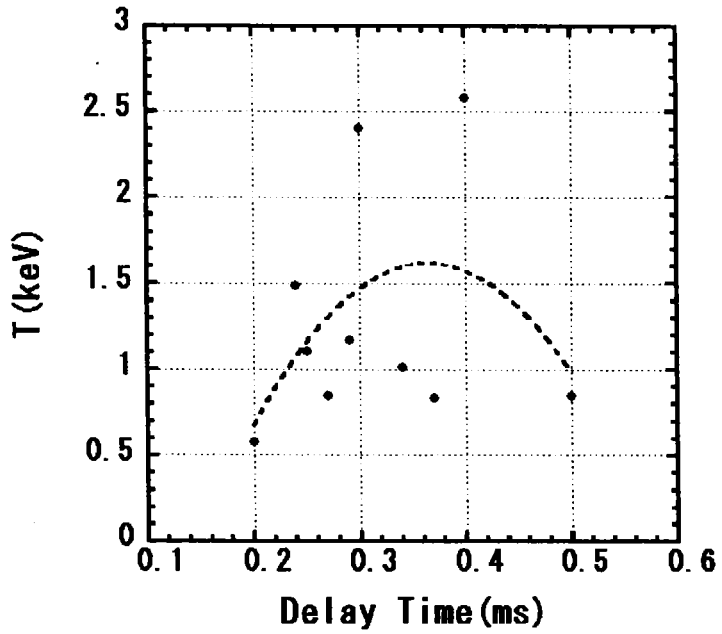

Fig. 9 Electron temperature vs. delay time.

V. Summary

The characteristics of x-ray radiation from the SHOTGUN gas-puff z-pinch plasma have been investigated by changing the delay time. Discharge cannot occur properly at the delay time less than 0.2 ms. With the increase in the delay time both the pinch time and the pinch current increase, then the net input energy increases. At small delay time hard component of x-ray is observed, but hot spots are not produced, and the x-ray signal is weak. The cloud structure of x-ray image is intense in this operating region. The hot spots are effectively produced at larger delay time. The x-ray signal became intense as the delay time increased. Spectroscopic data shows that electron temperature has no significant differene by changing the delay time.

References

1) K. Takasugi, H. Suzuki, K. Moriyama, and T. Miyamoto: Jpn. J. Appl. Phys. **35**, 4051 (1996).
2) K. Takasugi, A. Takeuchi, H. Takada and T. Miyamoto: Jpn. J. Appl. Phys. **31**, 1874 (1992).
3) E.O. Baronova, K. Takasugi, V.V. Vikhrev and T. Miyamoto: Proc. 13th Int. Conf. High Power Particle Beams 784 (2001).
4) A.H. Gabriel and T.M. Paget: J. Phys. **B 5**, 673 (1972).
5) A.H. Gabriel: Mon. Not. R. astr. Soc. **160**, 99 (1972).
6) C.P. Bhalla: Mon. Not. R. astr. Soc. **172**, 359 (1975).